



Full Text View

[Volume 30, Issue 3 \(March 2000\)](#)

Journal of Physical Oceanography

Article: pp. 461–474 | [Abstract](#) | [PDF \(474K\)](#)

Velocity Probability Density Functions for Oceanic Floats

Annalisa Bracco

Istituto di Cosmogeofisica del CNR, Torino, Italy

J. H. LaCasce

IFREMER, Centre de Brest, Plouzane, France

Antonello Provenzale

Istituto di Cosmogeofisica del CNR, Torino, Italy

(Manuscript received June 29, 1998, in final form February 3, 1999)

DOI: 10.1175/1520-0485(2000)030<0461:VPDFFO>2.0.CO;2

ABSTRACT

Probability density functions (PDFs) of daily velocities from subsurface floats deployed in the North Atlantic and equatorial Atlantic Oceans are examined. In general, the PDFs are approximately Gaussian for small velocities, but with significant exponential tails for large velocities. Correspondingly, the kurtoses of the distributions are greater than three. Similar PDFs are found in both western and eastern regions, above and below 1000-m depth, with more significant non-Gaussianity in the North Atlantic than at the equator. Analogously, Lagrangian statistics in decaying two-dimensional turbulence also display non-Gaussian velocity PDFs with approximately exponential tails, in the limit of large Reynolds number.

1. Introduction

The statistical analysis of ocean float data is often made in terms of a presumed advective–diffusive balance in the horizontal. [Davis \(1987\)](#) set the framework for such an analysis by showing how an advective–diffusive transport equation could be derived from single particle statistics. Examples of the application of these ideas are [Davis \(1985\)](#), [Brink et al. \(1991\)](#), and [Swenson and Niiler \(1996\)](#); recent modifications include the use of stochastic particle models to obtain improved estimates of diffusivities (e.g., [Griffa et al. 1995](#)). Central to this application is the

Table of Contents:

- [Introduction](#)
- [Data](#)
- [Results](#)
- [Barotropic turbulence](#)
- [Discussion](#)
- [REFERENCES](#)
- [TABLES](#)
- [FIGURES](#)

Options:

- [Create Reference](#)
- [Email this Article](#)
- [Add to MyArchive](#)
- [Search AMS Glossary](#)

Search CrossRef for:

- [Articles Citing This Article](#)

Search Google Scholar for:

- [Annalisa Bracco](#)
- [J. H. LaCasce](#)
- [Antonello Provenzale](#)

assumption that Lagrangian velocity departures from the local mean velocities are “quasi-Gaussian,” or nearly normal (Davis 1987).

However, this need not be the case in large-scale geophysical flows, where long-lived vortices and meandering jets may produce the type of flow organization that yields deviations from normal statistics. Evidence from high-resolution numerical experiments are indeed suggestive of non-Gaussian behavior. Simulations of barotropic turbulence and of point vortices (Weiss et al. 1998; Bracco et al. 1999, Manuscript submitted to *Phys. Fluids*) yield velocity probability density functions (PDFs) that are not Gaussian but are better described by either exponential or power-law distributions. The same was true of particles in the experiments described by Solomon et al. (1993). However, such highly idealized systems need not be representative of the ocean or atmosphere.

Perhaps surprisingly, PDFs have rarely been calculated from float or balloon trajectories; when they were, the results were mixed. Swenson and Niiler (1996) found that PDFs of velocities from surface drifters off California were by and large Gaussian, after binning and normalizing the data in small areal boxes to correct for lateral flow inhomogeneities. Others have looked at the statistics of relative (two-particle) velocities: Peskin and Peskin (1981) found that the relative displacements of balloons at 150 mb in the Southern Hemisphere were non-Gaussian, and Davis (1985) found that the relative displacements of surface drifters off California have a nonnormal distribution for small initial separations.

In this work, we calculate single particle velocity PDFs from a large number of subsurface float trajectories in the North and equatorial Atlantic. We show that the associated Lagrangian velocity PDFs depart from a Gaussian distribution, primarily due to an excess of energetic events, which yield nearly exponential wings. Interestingly, we find similar velocity PDFs in freely decaying barotropic turbulence simulations.

The rest of the paper is organized as follows. The dataset is discussed first. The velocity distributions are presented thereafter, for the western and eastern North Atlantic, and for the equatorial Atlantic. Afterward, we present PDFs obtained from simulations of decaying two-dimensional turbulence. A discussion of the findings concludes the work.

2. Data

Float velocities were calculated from trajectories archived at the World Ocean Circulation Experiment Subsurface Float Data Assembly Center at Woods Hole. These represent primarily SOFAR and RAFOS floats, most of which were deployed in the North and equatorial Atlantic. As such, our results pertain to these regions, although we suspect the findings may be generic to the subsurface ocean. The float experiments, relevant references, and the number and location of the floats are given in Table 1.

In the table, WA and EA refer to the western and eastern Atlantic respectively, and Eq to the equatorial Atlantic. In addition, we separated floats in the main thermocline (nominally taken to be depths $\lesssim 1000$ m) and those below. If a given experiment had floats at both levels, the first (second) number represents the number of floats above (below) the thermocline; experiments with floats only at one level are indicated. Only float records longer than one week were used. The trajectories in the two depth classes are shown in Fig. 1.

Float positions were converted to daily velocities by center differencing (although single differencing yields the same results). In some cases, float positions were recorded more frequently than once a day, and these records were averaged to yield daily positions prior to the center differencing. PDFs are presented for the three regions (western, eastern, and equatorial Atlantic), in the two depth ranges (above and below 1000 m), for both zonal and meridional velocities.

3. Results

a. Western North Atlantic

We begin with the floats to the west of the mid-Atlantic Ridge in the North Atlantic. Binning the zonal and meridional velocities of floats shallower than 1000 m into 2 cm s^{-1} wide velocity classes yields the histogram in the upper panel of Fig. 2, and binning the data from floats deeper than 1000 m into 1 cm s^{-1} wide classes yields the histogram in the lower panel.

At both depth levels, the PDFs are strongly non-Gaussian. Superimposed on the plots are two distributions for comparison; the dashed line indicates a Gaussian distribution:

$$f(u) = \frac{1}{\sqrt{2\pi}\sigma} \exp(-u^2/2\sigma^2), \quad (1)$$

whereas the solid line is an *exponential* distribution:

$$g(u) = \frac{1}{2u_*} \exp(-|u|/u_*). \quad (2)$$

The parameters σ and u_* were obtained by a least squares fit of the meridional velocity data at each depth. We observe that the distributions are closer to the exponential than to the Gaussian, although there are strong deviations for the positive velocities at shallower depths, and for the positive zonal velocities at depth. These deviations are reflected by positive values of skewness (the third-order moment) for the three distributions.

However, given the results of [Swenson and Niiler \(1996\)](#), we might expect departures from normality if the velocities are drawn from observations over too large an area. Indeed, it is well known that the North Atlantic has a mean flow and an eddy field that are greatly inhomogeneous (e.g., [Wunsch 1981](#)). So we recalculated the PDFs, as follows: velocities were grouped into 2° square bins, and the local means and standard deviations were calculated; the latter were then used to demean and normalize the original velocities. Finally, the normalized velocities u_n (which now have zero mean and unit variance) from all bins were recombined to yield PDFs for the whole region. Bins with fewer than 30 velocity realizations were discarded.

The results for the 37 658 velocity realizations in the deep western North Atlantic are shown in [Fig. 3](#). In the upper-left panel is the zonal velocity PDF, and the meridional velocity PDF is in the upper right. The PDFs have a smooth central core, like a Gaussian, but also have extended, nearly exponential, wings at large velocities. Calculating the kurtoses (the fourth-order moments) for the zonal and meridional (normalized) velocities yields 5.0 and 4.2, respectively, which are larger than the Gaussian value of 3. Note that, even for samples of only 1000 independent data extracted from a Gaussian distribution, the likelihood of finding a kurtosis larger than 3.5 is less than 0.004. So the values of the kurtosis obtained here indicate significant departures from Gaussianity.


A commonly used measure of goodness of fit is the Kolmogorov–Smirnov (K–S) test (e.g., [Priestley 1994](#); [Press et al. 1992](#)), which measures the significance of the maximum deviation between an empirical distribution and a specified theoretical one. The Lagrangian timescale at this depth is approximately 10 days, so there are approximately $37\,658/10 = 3766$ degrees of freedom. The K–S statistics are $\alpha = 0.0076$ and $\alpha = 0.019$ for the zonal and meridional velocity PDFs respectively, indicating rejection of the null hypothesis (that these samples are drawn from a normally distributed set) at the 95% confidence level. Of course, using fewer degrees of freedom yields somewhat larger values; for example, the significance for the zonal velocity rises to $\alpha = 0.049$ when a 15-day timescale is assumed. Nevertheless, these values are small and indicate a significant deviation from normality.

The deviation from normality is related to infrequent energetic events. In the lower panel of [Fig. 3](#) we show the location of those events for which the modulus of either the zonal or meridional normalized velocity, $|u_n|$, exceeds 3.5. These points are generally, though not always, clumped together. Sometimes they are clearly associated with swirling, eddylike trajectories, but other times with swift trajectories in a single direction over several days. Either way, the events are the result of coherent advection events, which in turn is suggestive of flow organization. Most occur near the western boundary, near the region of the southern recirculation of the Gulf stream.


If these events were only of single day duration, we might suspect that they were an artifact of errors in the float positioning (often on the order of several kilometers); if so, smoothing the trajectories would likely recover a Gaussian distribution. To check this, we recalculated the PDFs for the deep western Atlantic floats using 3-day and 5-day running mean velocities ([Fig. 4](#)). Shown in the upper panels are examples of one of the float's time series of zonal velocity with the running means. Note that the running means have substantially smaller velocity maxima. The PDFs for all the zonal velocities are shown below. We find the running mean distributions are somewhat more Gaussian, but still deviate in the wings. The kurtosis drops from $K = 5.0$ for the unsmoothed data to $K = 4.7$ for the 3-day mean to $K = 4.3$ for the 5-day mean. This suggests that some energetic events are shorter in duration than five days, but that many are actually longer. So the nonnormality is probably not a consequence of tracking errors. Similar PDFs are found in our turbulence simulations ([section 4](#)) where the particle positions are known with precision, which supports the assertion.

As noted, we normalized the data by subdividing into 2° boxes; how do the results change with different sized boxes? Shown in [Fig. 5](#) are the PDFs for the zonal and meridional velocities calculated from 1° , 2° , and 3° bins, and we observe that all the PDFs deviate from a Gaussian in the wings. The kurtoses for the respective zonal velocity pdf's are 4.4, 5.0, and 5.2, and for the meridional velocity PDFs 3.8, 4.2, and 4.7. The distributions are all nonnormal, although the PDFs calculated with smaller bins are closer to a Gaussian than those obtained with larger bins. On the other hand, the Lagrangian results from smaller bins are noisier, so the smaller bin PDFs have fewer total realizations and thus less statistical certainty. Henceforth we use the 2° bin, as a compromise between a smaller area and reasonable statistics. We come back to the issue

of flow inhomogeneities in the discussion section.


Above 1000 m in the western North Atlantic ([Fig. 6](#) ) we have 54 372 realizations, or about 50% more than below 1000 m. The zonal PDF is on the upper left, and the meridional PDF on the upper right. Again the PDFs are nonnormal, and the kurtoses (4.3 for the zonal, 4.5 for the meridional velocities) are significantly larger than 3. The Lagrangian timescales in the zonal and meridional directions are somewhat less than 10 days, but using 10 as a conservative estimate, the Kolmogorov–Smirnov test yields $\alpha = 2.5 \times 10^{-5}$ and $\alpha = 3.2 \times 10^{-5}$ for the zonal and meridional distributions, respectively.

The energetic events ($|u_n| > 3.5$) are plotted in the lower panel. Again there are many “clumped” or coherent events, although we note a larger number of single day events as well. The latter might be a consequence of shorter timescales of variability at this depth. Tracking errors peculiar to this depth range are also a possibility, though similar results are found at depth, and in other regions. Many of the energetic events ($|u_n| > 3.5$) occur south of the Gulf Stream, as with the deep data, but others lie in the region of the North Atlantic Current extension (e.g., Rossby 1998).


Thus we find similar distributions both in and below the main thermocline in the western Atlantic. The central portions of the PDFs appear approximately Gaussian, but the extended wings suggest an excess of energetic events. Note that the marked skewness noted in the regional PDFs of [Fig. 2](#)  is essentially remedied by the binning process, so the excess of positive velocity events seen there reflects inhomogeneous statistics.


b. Eastern North Atlantic

We perform the same analysis with float velocities from the eastern North Atlantic. There are fewer float trajectories in the east (perhaps due to the greater interest historically in the Gulf Stream region), but similar tendencies are evident.

As before, the data was binned in 2° boxes, demeaned and normalized by the local standard deviation before calculating the regional PDF. The results for the deep eastern Atlantic are shown in [Fig. 7](#) . Though there are fewer floats in the deep eastern Atlantic than in the deep western Atlantic, the trajectories are generally longer; so we have a comparable number of velocity realizations: 38 759. The PDFs here too are non-Gaussian, and the kurtoses are larger than in any other set: 6.6 for the zonal velocities and 5.8 for the meridional.


The Lagrangian timescales are somewhat longer than in the western Atlantic, but less than 15 days on average. Using 15 days, the Kolmogorov–Smirnov test yields $\alpha = 8.8 \times 10^{-4}$ and $\alpha = 0.002$ for the zonal and meridional distributions, respectively. Again one would reject the null hypothesis (of a Gaussian distribution) at the 95% (or even 99%) confidence level.

Plots of the positions of the energetic events (lower panel of [Fig. 7](#) ) display “clumping,” as in the west, but in this case the clumps can be traced to specific features, because many of the floats were intentionally deployed in “meddies.” The latter are anticyclonic vortices that emanate from the unstable outflow of the Mediterranean Sea (e.g., [Richardson et al. 1989](#)) and are thought to be important to the large-scale salinity distribution at depths from roughly 700 to 1500 m. The meddy floats loop rapidly, with periods on the order of several days.

In the shallow eastern Atlantic ([Fig. 8](#) ) there are only 13 502 realizations, but PDFs are also non-Gaussian and the kurtoses (4.0 in both cases) significantly larger than 3. The Lagrangian timescale here is between 10 and 15 days in both directions, but using 15, one obtains $\alpha = 0.19$ and $\alpha = 0.30$ for K–S statistics. Thus, one cannot reject a Gaussian distribution here, even though the kurtoses are elevated, but the higher values of α are related in part to the smaller number of points (which permits larger absolute deviations). As with the deep floats, the great majority of energetic events are due to floats deployed in meddies.

c. Equatorial Atlantic

The floats in the equatorial Atlantic subset come mostly from a single study, the Tropical Atlantic Experiment (e.g., [Richardson and Schmitz 1993](#)). As such, there are fewer velocity realizations here than in the North Atlantic, though fortunately a number of the floats drifted for many years. With 12 572 observations above 1000 m, and 20 889 below, we chose to lump all 33 461 observations together for the calculation. We used the same procedure of binning the velocities into 2° bins.

The PDFs ([Fig. 9](#) ) deviate from Gaussianity, but apparently less than in the previous cases. The kurtoses (3.7 for zonal, 3.6 for meridional velocities) are lower, and the K–S statistics are not small enough to reject the null hypothesis. The Lagrangian time scale is roughly 20 days in the zonal direction and 10 in the meridional direction (the dispersion is similarly anisotropic). Using these numbers to reduce the degrees of freedom, we find $\alpha = 0.13$ and $\alpha = 0.11$ for the zonal and

meridional distributions respectively. Unlike with the upper eastern Atlantic, one cannot dismiss these numbers for lack of data because the number of realizations is comparable to that in the deep western or eastern Atlantic. Thus, the extended wings are less significant here than in the other regions.

As before, most energetic events are of several days duration (lower panel), and one finds events that last longer than a week. Most occur near the western boundary, although the floats were also often deployed there. Two regions in particular stand out: the boundary near the equator and a region off the boundary near 7°N. The latter has been identified as a highly variable recirculation region ([Richardson and Fratantoni 1999, Manuscript in preparation](#)). The anomalous events generally involve fast translation in one direction rather than swirling, suggestive perhaps of jets or long waves rather than vortices.

4. Barotropic turbulence

The preceding results suggest an excess of energetic events over what one would have expected had the statistics been strictly normal. These events are often of several days duration, and apparently are related to specific oceanic features, for example, eddies or jets. As mentioned before, the role of tracking errors was a concern, so we wished to examine a system in which there is little uncertainty about the particles position, that is, in a model. We have chosen to analyze simulations of barotropic turbulence, where the accessible Reynolds numbers are higher than in larger scale ocean models. The results suggest similar Lagrangian PDFs, and so provide a first hint of the dynamical origin of non-Gaussian behavior.

The model we consider is based on the 2D Euler equation with biharmonic viscosity (e.g., [McWilliams 1984, 1990](#); [Provenzale 1999](#)):

$$\frac{\partial \omega}{\partial t} + [\psi, \omega] = -\nu \nabla^2 \nabla^2 \omega, \quad (3)$$

where $\omega = \nabla^2 \psi$ is relative vorticity, ψ is the streamfunction and

$$[A, B] = \frac{\partial A}{\partial x} \frac{\partial B}{\partial y} - \frac{\partial B}{\partial x} \frac{\partial A}{\partial y}$$

is the horizontal Jacobian. Particle advection in this system is performed by numerically solving the equations

$$\frac{dx}{dt} = -\frac{\partial \psi}{\partial y}, \quad \frac{dy}{dt} = \frac{\partial \psi}{\partial x}, \quad (4)$$

where $(x(t), y(t))$ is the particle position at time t and $(-\partial\psi/\partial y, \partial\psi/\partial x)$ is the Eulerian velocity at point (x, y) and time t . The Eulerian [equation \(3\)](#) is numerically integrated by using a standard pseudospectral collocation method ([Canuto et al. 1987](#)) with a third-order Adams–Bashforth time integration scheme and standard $2/3$ dealiasing.¹

In the simulations discussed below, we use periodic boundary conditions with domain size $L = 2\pi$ and resolution 512^2 grid points. We start with a random, Gaussian vorticity field with a narrowband initial spectrum, which evolves in time and forms well-defined coherent vortices ([McWilliams 1984](#)). After vortices have formed, 1024 passive particles are uniformly released into the flow. Their motion is then integrated by using the same temporal scheme and a third-order spectral spline interpolator. More details about these numerical simulations may be found in [Bracco et al. \(1999, Manuscript submitted to Phys. Fluids\)](#) and [Provenzale \(1999\)](#).

[Figure 10](#) shows the Lagrangian velocity PDFs obtained from the particle velocities. We have not binned the velocities as in the prior examples because the flows here are homogeneous. Two cases are shown: one in which the biharmonic diffusivity was $\nu = 5 \times 10^{-8}$ and a second in which the diffusivity was an order of magnitude smaller, $\nu = 5 \times 10^{-9}$. In the former case, the empirical distribution displays mild evidence of exponential wings, while in the latter case, the distribution has well-defined, strong exponential wings. Moreover, there are clear deviations from the Gaussian PDF even at small velocities; this is more clearly seen here than with the float data, due to the larger number of realizations. The respective kurtoses for the two cases are 3.9 and 4.2.

As noted above, the model affords many more velocity realizations. Even by taking just 20 velocity measurements for each particle (which gives 40 960 degrees of freedom), the Kolmogorov–Smirnov test gives $\alpha = 5 \times 10^{-2}$, and $\alpha = 5.5 \times 10^{-5}$, for the $\nu = 5 \times 10^{-8}$ and $\nu = 5 \times 10^{-9}$ cases, respectively. While we would not reject the null hypothesis at the 95% confidence level in the first case, we would in the second.

With a numerical model, we have more opportunity to explore the causes of the non-Gaussian distributions, and we do so in an accompanying work (Bracco et al. 1999, Manuscript submitted to *Phys. Fluids*). As mentioned, decaying turbulence such as this yields a population of long-lived vortices, but also a background field of vorticity that is stirred by the vortices. It appears that the non-Gaussian events occur in the region of the background turbulence between the vortices, and not in the vortices themselves. However, the vortices are important for the stirring and the creation of vorticity filaments, and in experiments without vortices the statistics are nearly normal. Analogously, the introduction of a strong β effect, which favors Rossby waves over coherent vortices, pushes the velocity PDFs toward a more Gaussian shape. These numerical results further confirm the view that, for float trajectories, non-Gaussian velocity PDFs are associated with the action of energetic coherent structures.

5. Discussion

The present results suggest that the PDF of Lagrangian velocities of subsurface floats in the North Atlantic is non-Gaussian. The observed values of the kurtosis, $4.0 \leq K \leq 6.6$, support this; so do low values of the Kolmogorov–Smirnov statistic, which indicate rejection of the null hypothesis at the 95% confidence level in most cases. The empirical distributions display extended wings for larger velocities that are more nearly exponential.

Similar results are obtained for PDFs calculated from passively advected particles in freely evolving barotropic turbulence. [Table 2](#) summarizes the values of the kurtosis and of the K–S significance level, α , for the dataset considered (for barotropic turbulence, no distinction between zonal and meridional directions has been made as the system is isotropic).

As can be seen in the table, two regions stand out as being more Gaussian: the upper eastern Atlantic and the equator. We have speculated that the larger K–S significance levels in the eastern Atlantic may be due to a paucity of data there, but this is clearly not the case at the equator.

The non-Gaussian nature of the velocity PDFs is presumably related to the presence of flow inhomogeneities. Note, however, that there are two quite different types of inhomogeneity: 1) geographical (lateral) inhomogeneities related to large-scale variations of the mean eddy kinetic energy and of other average quantities and 2) intrinsic dynamical inhomogeneities of mesoscale turbulence due to the fact that the turbulent field is composed of different dynamical regions that induce complex Lagrangian properties (see, e.g., [Elhmaidi et al. 1993](#) for a discussion of the intrinsic inhomogeneity of 2D turbulence). As discussed above, we have binned and normalized the float data in space to remove the effects of laterally inhomogeneous statistics. However, we did not bin the data in time, and spurious lateral inhomogeneities could still affect the PDFs if large-scale inhomogeneities had significantly changed their geographical position during the period spanned by the data. Removing this latter effect is difficult, as the data are too scarce to allow for a full binning in space and time. On the other hand, numerical simulation of barotropic turbulence, where large-scale inhomogeneities are of no concern, also indicate the presence of a non-Gaussian distribution with nearly exponential wings. That simulations of barotropic turbulence produce similar distributions to those observed with the floats gives us further confidence that the latter results are not simply the consequence of lateral inhomogeneities, but rather reflect the intrinsic dynamical inhomogeneity of mesoscale turbulence.

In light of these comments, one might speculate that the difference with equatorial PDFs, and possibly those from the shallow eastern Atlantic, is related to a lack of inhomogeneous features such as vortices. We noted earlier a difference in the character of “energetic” events among these floats (long translations as opposed to looping), which is consistent.

It is possible that non-normal PDFs could be the result of nonuniform deployments because the ocean is so inhomogeneous. It is certainly true that most float deployments are nonuniform in space as well as time. However, one notable exception was the EUROFLOAT Experiment at 1750 m in the eastern Atlantic in which floats were launched on a 2° grid ([Speer et al. 1998](#)). This region is less energetic than the western basin, and the floats do not loop anticyclonically like similar floats to the south in meddies. Normalizing the 20 030 velocity realizations from these floats in 2° bins and calculating the PDFs yields the distributions in [Fig. 11](#). As with the turbulence data ([Fig. 10](#)), deviations are found at both large and small velocities. The kurtoses in both directions are greater than 5, and K–S statistics suggest rejection of the null hypothesis at 95% confidence ([Table 2](#); a value of 15 days was used for the Lagrangian timescale, which is actually about 12 days in both directions here). So, a uniform deployment in this case yields the same results. Analogously, particle deployment in the turbulence simulations was also uniform.

It is known that Eulerian and Lagrangian spectra may be very different (e.g., [Babiano et al. 1987](#)), but Lagrangian and Eulerian velocity PDFs should coincide in the limit of dense, uniform sampling. This is the case with our turbulence simulations. But ocean observations are generally neither uniform nor dense, so one may well find differences between Eulerian and Lagrangian PDFs. Interestingly, satellite altimetry data suggests that oceanic surface velocities have nearly normal distributions over much of the ocean ([Gille and Llewellyn-Smith 2000](#)). The latter data have a much more uniform coverage than the subsurface floats; however, it’s possible that velocities in the surface layer where the wind exerts a direct

influence are more normal than at depth. As mentioned before, [Swenson and Niiler \(1996\)](#) found that surface drifters off California had velocity PDFs that also were essentially Gaussian. Whether ocean velocity PDFs vary in the vertical is unknown, but could be addressed by a systematic study of current meter velocities.

A final comment concerns the development and use of stochastic parameterizations of the Lagrangian motion of subsurface floats. The non-Gaussian shape of the velocity PDFs, if confirmed to be a general property of subsurface Lagrangian motions, indicates that simple linear stochastic models such as Brownian motion and the Orstein–Uhlenbeck process may not be appropriate to describe Lagrangian statistics in the ocean, as they yield velocity PDFs that are strictly Gaussian. Better parameterizations could presumably be based on the use of nonlinear stochastic models.

Acknowledgments

We are grateful to Tom Rossby for letting us use the North Atlantic Current float data, and to Kevin Speer and John Gould for the use of the EUROFLOAT data. We benefitted greatly from the comments of two anonymous reviewers, which motivated the more careful consideration of flow inhomogeneity effects, from discussions with Francesco Tampieri about empirical PDFs, and with Bach Lien Hua and Armando Babiano about flow inhomogeneities. We acknowledge support from the Programme “Transport Processes in the Atmosphere and the Ocean” of the European Science Foundation. JHL was supported under MAST PL920057 while at IFREMER in Brest, France.

REFERENCES

- Anderson-Fontana, S., and H. T. Rossby, 1991: RAFOS floats in the SYNOP Experiment: 1988–1990. University of Rhode Island, GSO Tech. Rep. 91-7, 155 pp. [Available online at <http://www.ntis.gov>.]
- Babiano, A., C. Basdevant, P. LeRoy, and R. Sadourny, 1987: Single-particle dispersion, Lagrangian structure function and Lagrangian energy spectrum in two-dimensional incompressible turbulence. *J. Mar. Res.*, **45**, 107–131..
- Brink, K. H., R. C. Beardsley, P. P. Niiler, M. Abbott, A. Huyer, S. Ramp, T. Stanton, and D. Stuart, 1991: Statistical properties of near-surface flow in the California coastal transition zone. *J. Geophys. Res.*, **96**, 14 693–14 706..
- Canuto, C., M. Y. Hussaini, A. Quarteroni, and T. A. Zang, 1987: *Spectral Methods in Fluid Dynamics*. Springer-Verlag, 576 pp..
- Cheney, R. E., W. H. Gemmill, M. K. Shank, P. L. Richardson, and D. Webb, 1976: Tracking a Gulf Stream ring with SOFAR floats. *J. Phys. Oceanogr.*, **6**, 741–749.. [Find this article online](#)
- Davis, R. E., 1985: Drifter observations of coastal surface currents during CODE: The statistical and dynamical view. *J. Geophys. Res.*, **90**, 4756–4772..
- , 1987: Modelling eddy transport of passive tracers. *J. Mar. Res.*, **45**, 635–666..
- Elhmaidi, D., A. Provenzale, and A. Babiano, 1993: Elementary topology of two-dimensional turbulence from a Lagrangian viewpoint and single-particle dispersion. *J. Fluid Mech.*, **257**, 533–558..
- Er-el, J., and R. Peskin, 1981: Relative diffusion of constant-level balloons in the Southern Hemisphere. *J. Atmos. Sci.*, **38**, 2264–2274.. [Find this article online](#)
- Gille, S. T., and S. G. Llewellyn Smith, 2000: Velocity probability density functions from altimetry. *J. Phys. Oceanogr.*, **30**, 125–136.. [Find this article online](#)
- Griffa, A., K. Owens, L. Piterbarg, and B. Rozovskii, 1995: Estimates of turbulence parameters from Lagrangian data using a stochastic particle model. *J. Mar. Res.*, **53**, 371–401..
- Leaman, K. D., and P. Vertes, 1994: Pathways in the Deep Western Boundary Current recirculation south of 30°N. University of Miami, RSMAS Tech. Rep. 94-002, 100 pp. [Available online at <http://www.ntis.gov>.]
- McWilliams, J. C., 1984: The emergence of isolated coherent vortices in turbulent flow. *J. Fluid Mech.*, **146**, 21–43..
- , 1990: The vortices of two-dimensional turbulence. *J. Fluid Mech.*, **219**, 361–385..
- Ollitrault, M., P. Tillier, I. Bodevin, and H. Klein, 1988: Deep SOFAR float experiment in the North-East Atlantic. Institut Francais de Recherche pour l’Exploitation de la Mer Tech. Rep. 11, 122 pp..

- Owens, W. B., 1984: A synoptic and statistical description of the Gulf Stream and subtropical gyre using SOFAR floats. *J. Phys. Oceanogr.*, **14**, 104–113.. [Find this article online](#)
- Press, W. H., S. A. Teukolshy, W. T. Vetterling, and B. P. Flannery, 1992: *Numerical Recipes in FORTRAN: The Art of Scientific Computing*. Cambridge University Press, 963 pp..
- Price, J. F., T. M. McKee, W. B. Owens, and J. R. Valdes, 1987: Site L SOFAR float experiment, 1982–1985. Woods Hole Oceanographic Institution Tech. Rep. WHOI-97-52, 289 pp. [Available online at <http://www.ntis.gov>.]
- Priestly, M. B., 1994: *Spectral Analysis and Time Series*. Academic Press, 890 pp..
- Provenzale, A., 1999: Transport by coherent barotropic vortices. *Annu. Rev. Fluid Mech.*, **31**, 55–93..
- Rees, J. M., and E. M. Gmitrowicz, 1989: Dispersion measurements from SOFAR floats on the Iberian abyssal plain. *Interim Oceanographic Description of the North-East Atlantic Site for the Disposal of Low-Level Radioactive Waste*. Vol. 3, F. Nyffeler and W. Simmons, Eds., Nuclear Energy Agency, OECD, 64–67..
- Richardson, P. L., and W. J. Schmitz Jr., 1993: Deep cross-equatorial flow in the Atlantic measured with SOFAR floats. *J. Geophys. Res.*, **98**, 8371–8387..
- , D. Walsh, L. Armi, M. Schroder, and J. F. Price, 1989: Tracking three Meddies with SOFAR floats. *J. Phys. Oceanogr.*, **19**, 371–383.. [Find this article online](#)
- Riser, S. C., and H. T. Rossby, 1983: Quasi-Lagrangian structure and variability of the subtropical western North Atlantic circulation. *J. Mar. Res.*, **41**, 127–162..
- Rossby, H. T., 1998: The North Atlantic current and surrounding waters: At the crossroads. *Rev. Geophys.*, **34**(4), 463–481..
- , A. D. Voorhis, and D. Webb, 1975: A quasi-Lagrangian study of mid-ocean variability using long-range SOFAR floats. *J. Mar. Res.*, **33**, 355–382..
- , S. C. Riser, and A. J. Mariano, 1983: The western North Atlantic—A lagrangian viewpoint. *Eddies in Marine Science*, A. R. Robinson, Ed., Springer-Verlag, 609 pp..
- , A. S. Bower, and P. T. Shaw, 1985: Particle pathways in the Gulf Stream. *Bull. Amer. Meteor. Soc.*, **66**, 1106–1110.. [Find this article online](#)
- , J. F. Price, and D. Webb, 1986: The spatial and temporal evolution of a cluster of SOFAR floats in the POLYMODE Local Dynamics Experiment (LDE). *J. Phys. Oceanogr.*, **16**, 428–442.. [Find this article online](#)
- Schmitz, W. J., Jr., J. F. Price, P. L. Richardson, W. B. Owens, D. C. Webb, R. E. Cheney, and H. T. Rossby, 1981: A preliminary exploration of the Gulf Stream system with SOFAR floats. *J. Phys. Oceanogr.*, **11**, 1194–1204.. [Find this article online](#)
- Solomon, T. H., E. R. Weeks, and H. L. Swinney, 1993: Observation of anomalous diffusion and Levy flights in a two-dimensional rotating flow. *Phys. Rev. Lett.*, **71**(24), 3975–3978..
- Speer, K. S., J. W. Gould, and J. H. LaCasce, 1998: Year-long trajectories of floats in Labrador Sea Water in the eastern North Atlantic Ocean. *Deep-Sea Res.*, **46**, 165–179..
- Sundermeyer, M. A., and J. F. Price, 1998: Lateral mixing and the North Atlantic Tracer Release Experiment: Observations and numerical simulations of Lagrangian particles and passive tracer. *J. Geophys. Res.*, **103**, 21 481–21 497..
- Swenson, M. S., and P. P. Niiler, 1996: Statistical analysis of the surface circulation of the California Current. *J. Geophys. Res.*, **101**, 22 631–22 645..
- Weiss, J. B., A. Provenzale, and J. C. McWilliams, 1998: Lagrangian dynamics in high-dimensional point-vortex systems. *Phys. Fluids*, **10**, 1929–1941..
- Wunsch, C., 1981: Low-frequency variability of the sea. *Evolution of Physical Oceanography*, B. A. Warren and C. Wunsch, Eds., The MIT Press, 342–375..
- Zenk, W., K. S. Tokos, and O. Boebel, 1992: New observations of meddy movement south of the Tejo plateau. *Geophys. Res. Lett.*, **19**, 2389–2392..
-

Tables

Table 1. Float experiments from which the present data were drawn. The numbers, region, and depth range of the floats in each group are indicated. WA: western Atlantic; EA: eastern Atlantic.

Experiment	Reference	Location	Number
Akkois Basin	Lemarié and Vautin (1994)	WA, deep	23
Eastern Basin	Richardson et al. (1989)	EA, deep	25
EUROFLOAT	Speer et al. (1996)	EA, deep	20
Gulf Stream	Schmitz et al. (1981)	WA	2, 3
Gulf Stream Rectification	Orvino (1984)	WA	26, 36
Iberian Basin	Ribe and Gostrowicz (1989)	EA, deep	6
IPM Basin Basin	Zank et al. (1992)	EA	30, 4
LDE	Rosby et al. (1986)	WA	23, 24
Long Range	Rosby et al. (1981)	WA, deep	3
MDEB	Rosby et al. (1975)	WA, deep	49
Neofouled Basin	Schmitz (1985)	WA	9, 3
North Atlantic Current	Rosby (1998)	EA	91, 1
Northwest Atlantic	Gillett et al. (1993)	EA, deep	14
Pre-LDE	River and Rosby (1983)	WA	40, 22
RACOS Pilot	Rosby et al. (1965)	WA	36, 4
RICE	Cheney et al. (1976)	WA	5, 4
Sun L	Price et al. (1987)	WA, shallow	33
Synop	Anderson and Rosby (1991)	WA	65, 3
Tropical Atlantic	Richardson and Schmitz (1993)	Eq	18, 36
Substation 1991	Sandomeyer and Price (1998)	EA, shallow	16
North Atlantic Tracer Release	Sandomeyer and Price (1998)	EA, shallow	8

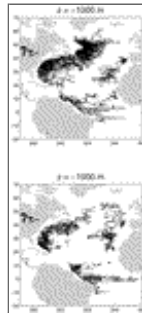
[Click on thumbnail for full-sized image.](#)

Table 2. Summary of the PDF statistics from this study, where K is the Kurtosis and α is the level of significance from the Kolmogorov–Smirnov test.

Dataset	Number of data points	K (zonal)	K (meridional)	α (zonal)	α (meridional)
WA, deep	37 658	5	4.2	0.0076	0.019
WA, shallow	54 372	4.3	4.5	0.000025	0.000035
EA, deep	38 759	6.6	5.8	0.00088	0.002
EA, shallow	13 502	4.3	4.5	0.19	0.30
Eq	33 461	3.7	3.6	0.13	0.11
EUROFLOAT	20 030	5.5	5.5	0.011	0.017
Turbulence	1 024 000	4.2		0.000055	

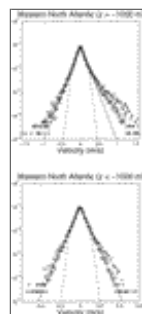
[Click on thumbnail for full-sized image.](#)

Figures



[Click on thumbnail for full-sized image.](#)

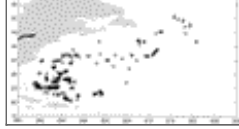
Fig. 1. Trajectories of the floats used in this study. Floats above 1000 m are at the top, and the deep floats at the bottom, as indicated.



[Click on thumbnail for full-sized image.](#)

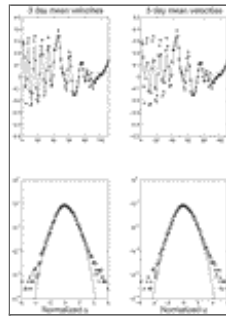
Fig. 2. The probability density functions for the velocities in the western Atlantic. The PDFs for the zonal velocities are indicated by (\times), and for the meridional velocities by (\circ). Also shown are the least squares best fit Gaussian curves (dashed lines) and exponential curves (solid lines).





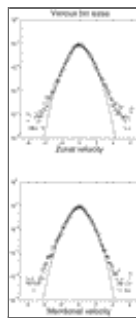
Click on thumbnail for full-sized image.

Fig. 3. PDFs of velocities from the deep western Atlantic. Velocities have been binned in 2° squares and normalized, as discussed in the text. The standard Gaussian PDF is indicated by the solid curve. In the lower panel are the locations of events where either the magnitude of the normalized zonal or meridional velocity exceeded 3.5.



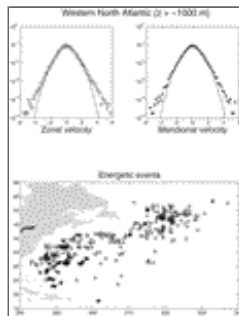
Click on thumbnail for full-sized image.

Fig. 4. PDFs of the zonal velocities from the deep western Atlantic with various degrees of trajectory smoothing. On the left, the velocities have been smoothed by a 3-day running mean, and on the right by a 5-day running mean. Examples of the resulting time series of velocity are shown in the upper panels, with the actual velocities in asterixes. Below are the PDFs; the actual PDFs are again indicated by asterisks, and the smoothed velocity PDFs by circles.



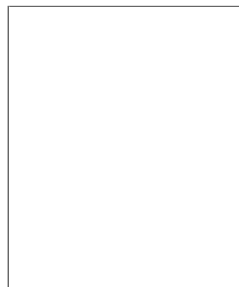
Click on thumbnail for full-sized image.

Fig. 5. The PDFs for the deep western North Atlantic using data normalized with various bin sizes. Shown are PDFs with 1° (points), 2° (\times 's) and 3° (\circ 's) bins.



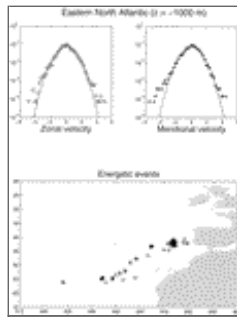
Click on thumbnail for full-sized image.

Fig. 6. The normalized velocity PDFs for the shallow western Atlantic. See the caption of [Fig. 3](#) for details.



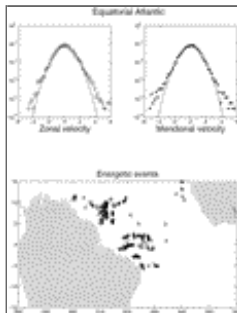
Click on thumbnail for full-sized image.

Fig. 7. The normalized velocity PDFs for the deep eastern Atlantic. See the caption of [Fig. 3](#) for details.



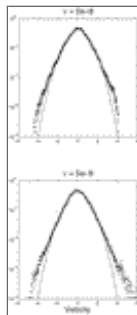
Click on thumbnail for full-sized image.

Fig. 8. The normalized velocity PDFs for the shallow eastern Atlantic. See the caption of [Fig. 3](#) for details.



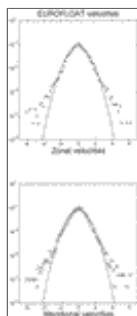
Click on thumbnail for full-sized image.

Fig. 9. The normalized velocity PDFs for the equatorial Atlantic. See the caption of [Fig. 3](#) for details.



Click on thumbnail for full-sized image.

Fig. 10. The PDFs for the Lagrangian velocities from two freely decaying barotropic turbulence solutions. The value of the biharmonic damping coefficients were as shown.



Click on thumbnail for full-sized image.

Fig. 11. The PDFs for the EUROFLOAT set. Velocities have been normalized after subdivision into 2° bins.

¹ The term “~~2/3~~ dealiasing” means that during the integration we constantly eliminate spectral power at wavenumbers larger than k_{\max} where $k_{\max} = \pi/\Delta x$ and Δx is the grid spacing. This is done to forbid the energy flowing from high wavenumbers to low wavenumbers (aliasing).

Corresponding author address: Joe LaCasce, WHOI MS 29, Woods Hole, MA 02543.

E-mail: jlacace@whoi.edu

top ▲



© 2008 American Meteorological Society [Privacy Policy and Disclaimer](#)

Headquarters: 45 Beacon Street Boston, MA 02108-3693

DC Office: 1120 G Street, NW, Suite 800 Washington DC, 20005-3826

amsinfo@ametsoc.org Phone: 617-227-2425 Fax: 617-742-8718

[Allen Press, Inc.](#) assists in the online publication of AMS journals.